Deexcitation of metastable Ba+

T. G. Walker and K. D. Bonin

Citation: The Journal of Chemical Physics **89**, 1358 (1988); doi: 10.1063/1.455187
View online: http://dx.doi.org/10.1063/1.455187
View Table of Contents: http://scitation.aip.org/content/aip/journal/jcp/89/3?ver=pdfcov
Published by the AIP Publishing

Deexcitation of metastable Ba^+

T. G. Walker and K. D. Bonin
Department of Physics, Princeton University, Princeton, New Jersey 08544

(Received 7 March 1988; accepted 18 April 1988)

This is a study of the deexcitation mechanisms of the metastable $5\,^2D_{3/2}$ state of Ba^+ in about 1 atm He buffer gas in the temperature range of 500–650 °C. The ions were produced by three-photon ionization with light tuned to a resonance between two excited states of Ba, enabling the electron density to be varied independently of the temperature and pressure. The deexcitation is dominated by superelastic scattering of electrons with a cross section of $\sigma_{se} = 45 \pm 20$ Å^2 (corresponding to an electron-impact excitation cross section of 11 Å^2) and quenching by Ba atoms with a cross section of $\sigma_{Ba} = 130 \pm 25$ Å^2. No dependence of the deexcitation rate on He density was detected, and we infer an upper limit on the cross section of $\sigma_{He} \leqslant 9 \times 10^{-22}$ cm^2.

I. INTRODUCTION

Recently there has been considerable interest in the deexcitation mechanisms of metastable states of important metal-vapor lasers, such as the copper-vapor laser[1] and the barium-vapor laser.[2] In both these lasers the slow deexcitation rates of the metastable states limit the laser efficiency. Also, in order to scale up the lasers to higher powers a knowledge of the physics of the metastable relaxation is required. An energy-level diagram for Ba^+ is shown in Fig. 1. Its structure is similar to both Ba and Cu, and lasing has been observed on its cross-fluorescent branches.[3] In addition, Ba^+ is a popular ion to study for many experiments because of its optical resonance lines. Clearly any experiment which utilizes the interaction of Ba^+ with resonance light from a lamp or laser will be affected by the deexcitation of the metastable states.

We report here measurements of the deexcitation rates of the $Ba^+(5\,^2D_{3/2})$ state in He buffer gas at densities of about 1 amagat and in the temperature range of 500–650 °C. We find that an important deexcitation mechanism is superelastic scattering with the electrons in the plasma, i.e.,

$$e^- + Ba^+(5\,^2D_{3/2}) \rightarrow e^- + Ba^+(6\,^2S_{1/2}) + \Delta E, \quad (1)$$

where $\Delta E = 4674$ cm^{-1} is the excitation energy of the $Ba^+(5\,^2D_{3/2})$ state. Using the principle of detailed balance, we deduce an electron-impact excitation cross section of 11 ± 4.9 Å^2. After subtracting off the contribution of superelastic collisions, we find that the remainder of the deexcitation is due to collisions with neutral Ba atoms, i.e.,

$$Ba + Ba^+(5\,^2D_{3/2}) \rightarrow Ba + Ba^+(6\,^2S_{1/2}) + \Delta E, \quad (2)$$

and we obtain a cross section of $\sigma_{Ba} = 130 \pm 25$ Å^2. This large cross section is reasonable due to the low energy of the $5\,^2D_{3/2}$ state and the repulsive nature of the lowest $^2\Sigma_g^+$ potential curve of Ba_2^+. Finally, we observe no dependence of the deexcitation rate on the He density, and we infer an upper limit on the deexcitation cross section of $\sigma_{He} \leqslant 9 \times 10^{-22}$ cm^2.

II. CREATION AND DETECTION OF Ba^+

In order to study Ba^+ in He as unambiguously as possible, we produced the Ba^+ by photoionization. This allowed for variation of the electron density independent of the He density or the Ba density.

An efficient way to photoionize Ba is to use a multiphoton process with one or more resonant intermediate steps. For this experiment the doubled output of a Nd:YAG laser ($\approx$250 mJ/8 ns) was used to pump a rhodamine 590 tunable dye laser (bandwidth $\approx$15 GHz). Energies of up to 100 mJ/pulse were obtained at 5513 Å, the wavelength corresponding to the $6s6p\,^1P_1$–$5d\,6d\,^3D_2$ transition in Ba (see Fig. 2). Although this is not resonant with any atomic Ba transitions originating with the Ba ground state, a large amount of visible fluorescence was observed when this light was put into an oven (described in Ref. 4) containing Ba vapor and He gas at a temperature of 500–600 °C. This fluorescence was found to be due to neutral Ba transitions, the strongest of which have the $5d\,6d\,^3D_2$ state for the upper state, although many transitions from other states were observed. The duration of the fluorescence was about 500 ns. Metastable Ba^+ ions were

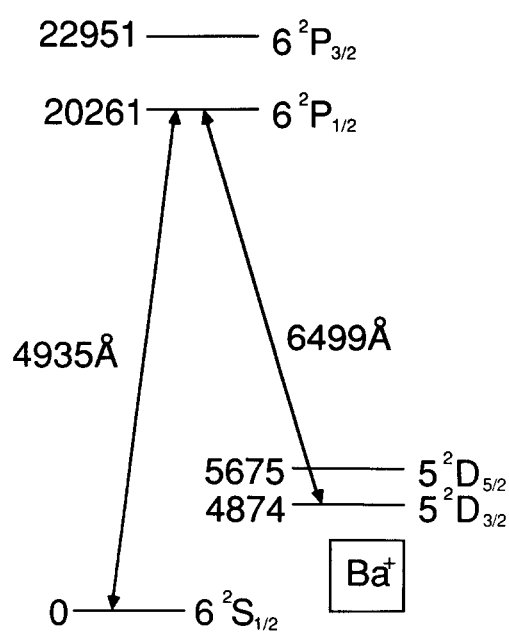

FIG. 1. Low-lying states of Ba^+. Energies are in cm^{-1}.

 0021-9606/88/151358-06$02.10

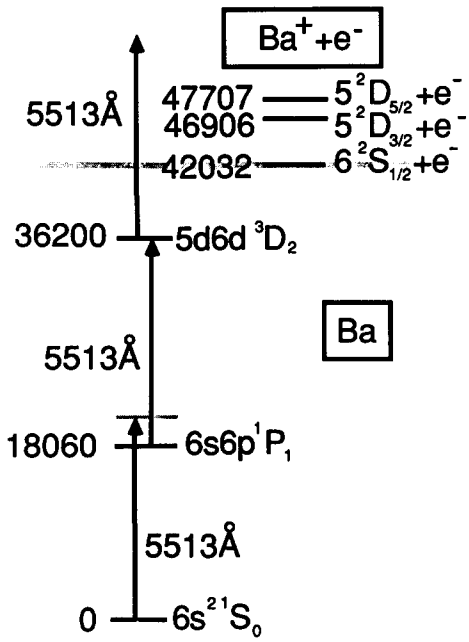

FIG. 2. Energy levels relevant to the Ba photoionization process. Energies are in cm^{-1}.

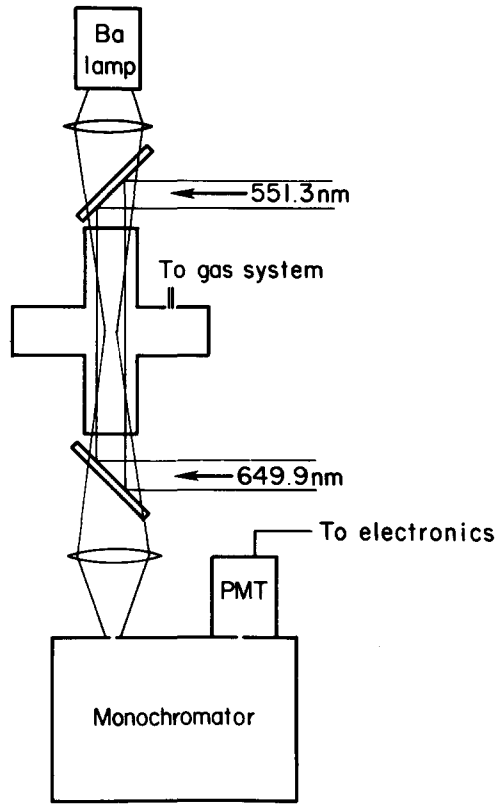

FIG. 3. Arrangement to measure the processes in a Ba^+ plasma in He buffer gas.

readily observed by exciting the $Ba^+ 5\,^2D_{3/2}$–$6\,^2P_{1/2}$ transition with a tunable dye laser and observing the resulting 4935 Å fluorescence due to the $6\,^2P_{1/2}$–$6\,^2S_{1/2}$ transition. Estimates of the ion density will follow later in this section.

The efficiency of the above photoionization process increases with increasing He pressure, suggesting that the ionization mechanism is as follows. Ground state Ba atoms absorb a photon during a collision with a He atom. The resulting BaHe excited state then dissociates or is broken up in a collision with another He atom, leaving the Ba atom in the $6s6p\ ^1P_1$ state. The $6s6p\ ^1P_1$–$5d\,6d\ ^3D_2$ transition is easily saturated by the resonant laser light. Finally ionization occurs with the absorption of a third laser photon from the $5d\,6d\ ^3D_2$ level.

The experimental setup is shown in Fig. 3. As mentioned above, the pulsed dye laser output at 5513 Å ionized the hot Ba vapor in the center of the oven. A barium hollow-cathode lamp, the absorption of which served to measure the $Ba^+ 6\,^2S_{1/2}$ density, was focused into the cell through a dichroic mirror. Upon exiting the cell another dichroic mirror separated the laser from the lamp, and the lamp was focused onto the slits of a 0.3 m monochromator, which isolated the 4935 Å resonance line and prevented saturation of the photodetector by the strong atomic fluorescence at other wavelengths in the first 500 ns after the laser pulse. To detect the $Ba^+ 5\,^2D_{3/2}$ state directly a cw dye laser ($\approx$1 mW) was tuned to the $Ba^+ 5\,^2D_{3/2}$–$6\,^2P_{1/2}$ transition at 6499 Å and the resulting fluorescence at 4935 Å was detected in the same manner as the lamp. This laser beam was also reflected into the cell by the dichroic mirror. The output of the photomultiplier tube mounted at the output slit of the monochromator was fed to an amplifier of bandwidth 300 kHz and sent to a transient digitizer/signal averager. The resulting waveforms were then analyzed using a microcomputer.

Two measurements of importance for the experiments were the Ba number density and the electron number density. The Ba number density was determined by measuring the temperature of the cell with a chromel/alumel thermocouple and using the known vapor pressure curves[5] to obtain the number density. This procedure was confirmed by measuring the Faraday rotation[6] of light near the Ba 5535 Å reonance in an 800 G magnetic field at a wide range of He pressures. The results were consistent with the vapor pressure curves.

The electron density in the Ba^+ plasma was determined as follows. Since the Debye length for the conditions of this experiment was on the order of 10 μ, charge neutrality of the plasma held to a good approximation. The absorption of the hollow-cathode light at 4935 Å after the $5\,^2D_{3/2}$ state population had decayed to the $6\,^2S_{1/2}$ state thus gave the electron density, assuming a knowledge of both the lamp profile and the absorption profile of the $Ba^+ 6\,^2S_{1/2}$ states. To determine the lamp profile, a scanning confocal Fabry–Perot etalon (FSR 7.5 GHz, finesse$\approx$200) was used to measure the line shape (Fig. 4). The background was assumed to be from light far removed from the resonance. This assumption was validated by producing enough ions to saturate the absorption of the on-resonant component of the lamp light. The observed absorption was 45%, in agreement with the area of the background in Fig. 4.

The line shape of the $Ba^+\ 6\,^2S_{1/2}$–$6\,^2P_{1/2}$ transition was also required. The absorption cross section $\sigma_B(\nu)$ at the He pressures of this experiment (250–1000 Torr) should be well represented by a pressure-broadened Lorentzian:

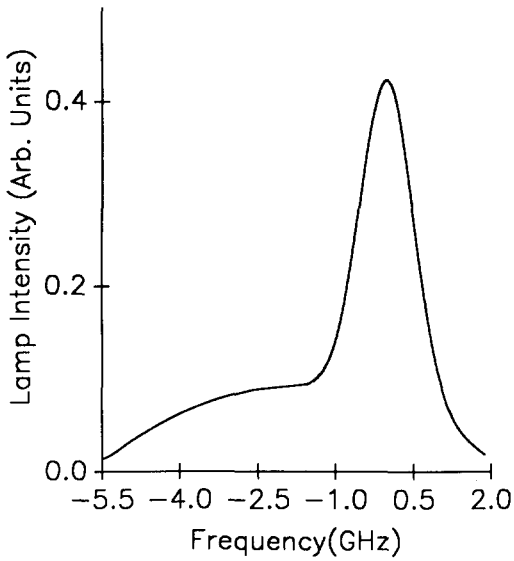

FIG. 4. The hollow-cathode lamp profile of the Ba^+ $6\,^2P_{1/2}$–$6\,^2S_{1/2}$ line at 4935 Å as observed by a scanning confocal Fabry–Perot etalon. The slowly varying background was assumed to be from wavelengths far removed from 4935 Å.

$$\sigma_B(\nu) = \frac{r_e f c \gamma_B/2}{(\nu - \nu_0 - \beta_B)^2 + \gamma_B^2/4}. \tag{3}$$

Here γ_B and β_B are the broadening (FWHM) and shift parameters for the transition at a given He pressure, r_e is the classical electron radius, $f = 0.35$ the oscillator strength for the transition,[7] and ν_0 the unshifted frequency of the transition. γ_B and β_B have not been measured for Ba^+ broadened by He, but reasonable estimates can be made in the following manner. Table I shows the measured values of $\gamma_B/[\mathrm{He}]$ for the alkaline–earth ions Mg^+, Ca^+, and Sr^+ at 550–650 °C. The broadening parameter is the same for Ca^+ and Sr^+, implying that a value for $\gamma_B/[\mathrm{He}]$ of 8.9 GHz/amagat is probably reasonable for Ba^+. The shift parameter does not behave so conveniently, but Fig. 5 shows that it increases monotonically from Mg^+ to Sr^+, so a reasonable value obtained from Fig. 5 is 7.8 GHz/amagat.

With the lamp profile $I_l(\nu)$ and the ionic line shape $\sigma_B(\nu)$ determined as described above, the Ba^+ number density n was obtained from the measured absorption A by

$$A = \int I_l(\nu)\exp[-n\sigma_B(\nu)l]\,d\nu. \tag{4}$$

Here the path length l was estimated to be about 5 cm for the cell. $Ba^+6\,^2S_{1/2}$ state number densities obtained in this way were as large as 7×10^{11} cm^{-3}. Clearly the major uncertainty here is the unknown shift parameter. More will be said about this in Sec. III.

TABLE I. Pressure broadening parameter for the principal $^2S_{1/2}$–$^2P_{1/2}$ transition in the alkaline–earth ions broadened by He as measured by Giles and Lewis (Ref. 8).

Ion	Broadening parameter
Mg^+	15.4 GHz/amagat
Ca^+	8.9 GHz/amagat
Sr^+	8.9 GHz/amagat

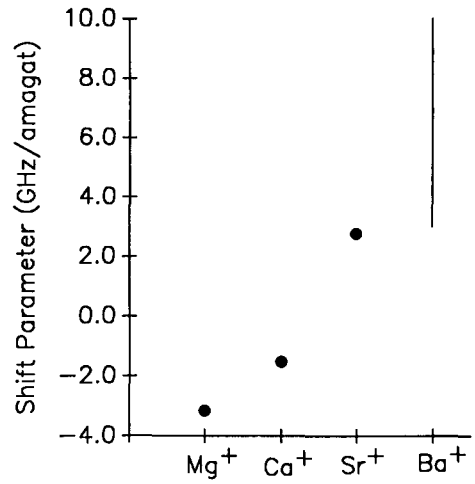

FIG. 5. Measured values of the shift parameter $\beta_B/[\mathrm{He}]$ for the alkaline–earth ions Mg^+, Ca^+, and Sr^+. For Ba^+ the solid line denotes the range of values assumed in the data analysis (1 amagat $= 2.69\times10^{19}$ cm^{-3}).

III. DEEXCITATION RATE MEASUREMENTS

A typical type dependence of the $Ba^+5\,^2D_{3/2}$ state is shown in Fig. 6. The $5\,^2D_{3/2}$ state population was maximum shortly after the ionization was produced by the laser, then decayed exponentially to zero.

Figure 7 shows the $5\,^2D_{3/2}$ state deexcitation rate vs electron number density (as determined from the absorption of the hollow cathode lamp), at fixed temperature and pressure. This suggests that superelastic scattering of electrons is an important deexcitation mechanism for the $5\,^2D_{3/2}$ state. Assuming this to be the mechanism, the slopes of curves like Fig. 7 give the cross section for superelastic scattering. The main difficulty, as explained before, is the calibration of the

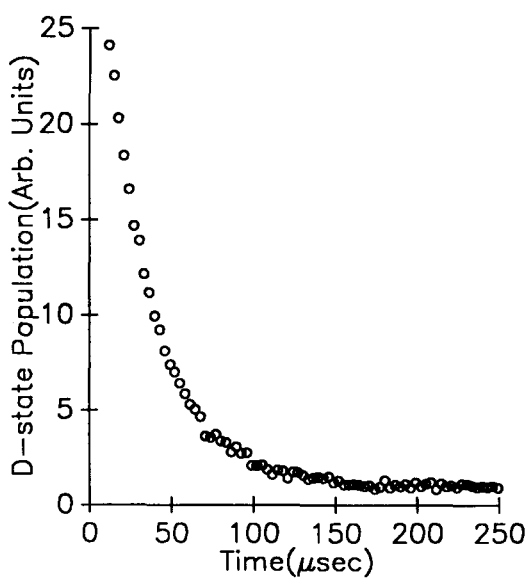

FIG. 6. $Ba^+5\,^2D_{3/2}$ population as a function of time after the photoionization laser pulse. The $5\,^2D_{3/2}$ states are detected by tuning a cw dye laser to the $5\,^2D_{3/2}$–$6\,^2P_{1/2}$ transition at 6499 Å, and observing the intensity of the resulting fluorescence at 4935 Å. The fluorescent intensity is plotted on the vertical axis.

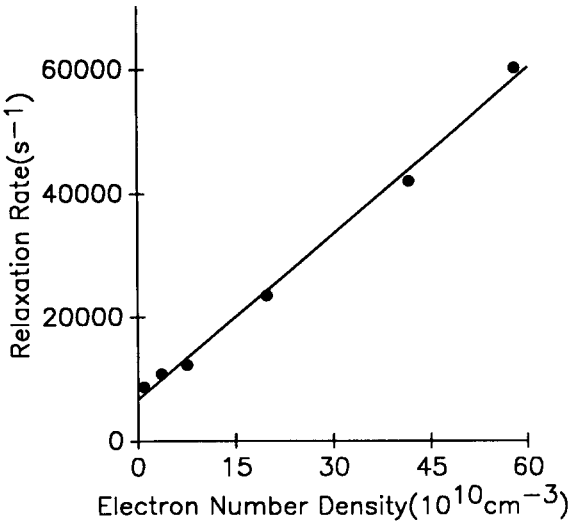

FIG. 7. Deexcitation rate of $Ba^+ 5\,^2D_{3/2}$ state as a function of the electron density deduced from the absorption of the hollow-cathode lamp.

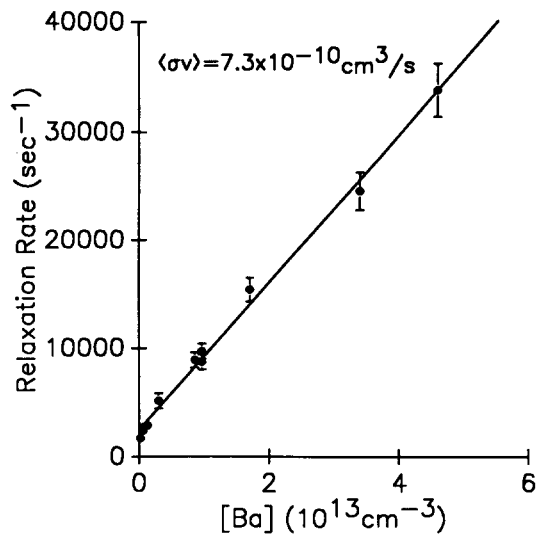

FIG. 8. Deexcitation rate in the absence of electrons as a function of Ba number density. The number density was determined from the cell temperature using published vapor pressure curves (Ref. 5).

electron density scale, which requires assumptions concerning the pressure broadened and shifted absorption profile of the ions. For this reason, the data were analyzed assuming several different values for the shift parameter. The results are shown in Table II. A reasonable value for the cross section, from Table II, is approximately 45 $Å^2$ with conservative error bars of 20 $Å^2$. This result will be discussed in Sec. IV.

The existence of a nonzero intercept in Fig. 7 suggests that some quenching process from atoms or molecules in the vapor contributed to the deexcitation. If the quenching species is He, the intercept would depend linearly on the pressure. No pressure dependence of the deexcitation rate was observed over a pressure range of 0.5 atm with a sensitivity of 1000/s at 550 °C. This establishes an upper limit on the cross section for quenching by He of $\sigma_{He} \leqslant 9\times10^{-22}\ cm^{-3}$.

The temperature dependence of the intercept was also studied experimentally. An Clausius–Clapeyron-type dependence, i.e., rate$\sim\exp(-U/kT)$ of the intercept on temperature was observed, with $U = 1.7 \pm 0.2$ eV. The latent heat of vaporation of Ba is 1.8 eV,[5] suggesting that the dominant deexcitation mechanism responsible for the temperature dependence is collisions with neutral Ba atoms. Assuming this to be the case, we show in Fig. 8 the deexcitation rate at zero electron density, i.e., the intercepts of curves like Fig. 7, plotted as a function of the Ba density. The slope of the line gives the cross section to be $\sigma_{Ba} = 130 \pm 25$ $Å^2$. This result will be compared with other measurements in Sec. IV.

TABLE II. Experimental superelastic cross sections deduced using different values of the shift parameter.

Shift parameter (GHz/amagat)	Superelastic cross section ($Å^2$)
3.0	74
5.25	53
7.9	39
10.0	22

It is possible that other species in the cell contributed to the results of Fig. 8. One possibility is molecular impurities. Ba is well known to be an efficient getter for impurities, with the important exception of H_2. At 600 °C, the dissociation pressure of BaH_2 is 10^{-3} atm.[10] Thus, if a significant amount of hydrogen is dissolved in the Ba metal in the cell, a substantial hydrogen pressure will exist in the cell. Indeed, when the experiment was begun the measurements of the intercept were larger than shown in Fig. 8. The existence of hydrogen in the cell was confirmed by replacing the He by Kr and observing the Balmer α line in H when the doubled Nd:YAG was focused into the cell, ionizing the gas (the Kr gas was necessary because no spark could be obtained with He). The Balmer α line was the strongest feature in the spectrum. The H_2 density was then reduced by cleaning the cell, replacing the Ba metal (which had been loaded one year before) with fresh Ba, and inserting a commercial getter (Zr–V–Fe, quoted H_2 vapor pressure of 10^{-16} Torr at room temperature) into the cooled side arms of the cell. The experiment with the laser produced spark was then repeated, and no Balmer α line was observed. A decrease in the deexcitation rate to the values of Fig. 8 also occurred, indicating that H_2 had been contributing to the $Ba^+\ ^2D_{3/2}$ quenching, but was eliminated by the fresh Ba and the getter.

The main impurities in the Ba rod were reported by the supplier to be the alkalis and Sr. An upper limit on the alkali density was obtained by looking for absorption of the resonance lines. None was seen with a sensitivity of about 10^{-4} of the Ba absorption, so the alkali densities were insignificant. The Sr density was measured by the Faraday rotation technique to be less than the Ba density by a factor of 4, and so Sr may have contributed to the quenching. The cross section should be smaller for Sr than for Ba, however, as will be discussed in Sec. IV, so the correction will be assumed to be negligible.

A small intercept also exists in Fig. 8. This contribution to the quenching could be the result of some species whose

density was not dependent on the pressure or temperature of the cell, but was not investigated further.

IV. DISCUSSION OF Ba^+ QUENCHING MECHANISMS

The superelastic cross section measurement discussed in Sec. II can be related by detailed balance to the cross section for electron-impact excitation from the $6\,^2S_{1/2}$ state to the $5\,^2D_{3/2}$ state.[11] This gives the relation

$$g_S v^2 Q_{ei}(v) = g_D v'^2 Q_{se}(v'), \tag{5}$$

where Q_{ei} is the electron-impact excitation cross section, Q_{se} is the superelastic cross section, g_s and g_D are the statistical weights of the $6\,^2S_{1/2}$ and $5\,^2D_{3/2}$ states, and the velocities v and v' are related by conservation of energy:

$$v^2 = \frac{2E_D}{m} + v'^2. \tag{6}$$

Here E_D is the excitation energy of the $5\,^2D_{3/2}$ state.

The measured superelastic rate constant is the average of $Q_{se}v'$ over the electron distribution function $f(v')$:

$$\langle Q_{se}v'\rangle = \int f(v')Q_{se}(v')v'd^3v'$$

$$= \frac{g_S}{g_D}\int \frac{f(v')}{v'} v^2 Q_{ei}(v)d^3v'. \tag{7}$$

Electron-ion impact excitation cross sections obey $Q_{ei}v^2 = \text{const}$ near the threshold for a given transition,[12] so $Q_{ei}v^2$ can be factored out of the integral in Eq. (7), giving

$$\langle Q_{se}v'\rangle = \frac{g_S}{g_D}\frac{2E_D Q_{ei}}{m}\int \frac{f(v')}{v'} d^3v'$$

$$= \frac{g_S}{g_D}\frac{4E_D Q_{ei}}{(2\pi mkT)^{1/2}}. \tag{8}$$

The measured cross section was obtained from $\langle Q_{se}v'\rangle$ by the relation

$$\sigma_{se} = \frac{\langle Q_{se}v'\rangle}{(8\ kT/\pi m)^{1/2}} = \frac{g_S}{g_D}\frac{E_D}{kT}Q_{ei}. \tag{9}$$

For $\sigma_{se} = 45$ Å^2, this gives $Q_{ei} = 11$ Å^2 for excitation of the $5\,^2D_{3/2}$ state. Petrini[13] has calculated $Q_{ei} = 25$ Å^2 for the sum of the $6\,^2S_{1/2}$–$5\,^2D_{3/2}$ and $6\,^2S_{1/2}$–$5\,D_{5/2}$ cross sections so, assuming the separate cross sections scale by their statistical weights, his calculation gives $4/10\times 25$ Å$^2 = 10$ Å^2, in excellent agreement with this experiment. This is perhaps fortuitous, since the calculations of Petrini neglected the Ba^+ fine structure and the experimental determination of the electron number density is subject to error of about a factor of 2.

The large quenching (130 Å^2) of $Ba^+ 5\,^2D_{3/2}$ by Ba can be understood with the aid of Fig. 9, which shows the two lowest potential curves of Ba_2^+ as calculated by Sramek,[14] as well as a potential curve correlating at large internuclear separations with the $5\,^2D_{3/2}$ state obtained by displacing the $^2\Sigma_u^+$ potential by the $5\,^2D_{3/2}$ excitation energy, 4674 cm^{-1}. The repulsive nature of the $^2\Sigma_g^+$ means that a curve crossing can occur at relatively large internuclear separation with a potential curve from the $5\,^2D_{3/2}$ states. Setting the experimental cross section equal to πR^2, where R is the internuclear separation at which the crossing occurs, gives $R = 6$ Å, which is very close to the crossing in Fig. 9 obtained by crude methods. Another measurement of this cross section was made by Bokhan,[16] who obtained a cross section of $\sigma_{Ba} = 200 \pm 40$ Å^2. This measurement may be too high because of neglect of electron superelastic scattering. Interestingly, the cross section for the quenching of the Ba metastable states has been measured[15] to be 130 Å^2, even though there is no highly repulsive ground state potential in Ba_2. The strong quenching in Ba_2 has been attributed by Jones[17] to be due to extremely strong attraction of the metastable potentials.

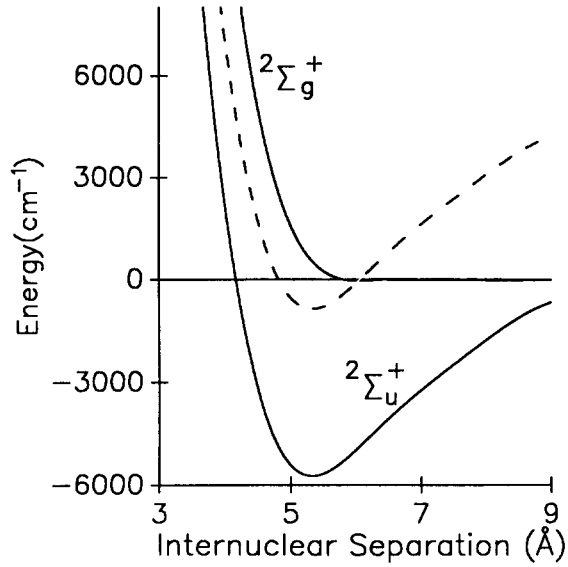

FIG. 9. Potential curves for low-lying states of Ba_2^+. The solid lines are the potentials calculated by Sramek (Ref. 14) and the dashed line is an excited potential obtained by displacing the $^2\Sigma_u^+$ curve by the $5\,^2D_{3/2}$ excitation energy.

In contrast to Ba_2^+, for $SrBa^+$ there is no repulsive potential curve which asymptotically goes to a free Ba^+ and a free Sr atom. Thus any curve crossings between the ground state potential of $SrBa^+$ and potentials correlating to the $5\,^2D_{3/2}$ state of Ba^+ will most likely be at small internuclear separations, with resulting small quenching cross sections. For this reason Sr quenching is assumed to have a negligible contribution to the cross sections reported in Sec. III.

The lack of observed quenching of $Ba^+(D)$ by He is in apparent conflict with the interpretation of Schneider and Werth[18] of the He pressure dependence of the lifetime of $Ba^+(D)$ in an ion trap. In these experiments the He atoms acted to thermalize Ba^+ created by surface ionization on a Pt filament. After the Ba^+ ions were trapped, the gas was pumped away. These experiments exhibited a linear dependence of the $Ba^+(D)$ lifetime on the total residual pressure. If the quenching agent was He, the deduced cross section is 6×10^{-17} cm^2, almost five orders of magnitude larger than the upper limits found in Sec. III. A possible explanation for this disagreement is that in the ion trap experiments impurities produced by the hot filament and the hot source of Ba atoms mixed with the He buffer gas. Then the residual gas had a small impurity content, perhaps H_2. If a quenching cross section for the impurities of 1×10^{-14} cm^2 is assumed

the impurity concentration required to explain the quenching is about 1%. At the small He pressures used (10^{-9} bar) this implies an impurity density of only 10^8 cm^{-3}.

Another difficulty of the cross section deduced from Schneider and Werth's paper is in explaining the physical process producing the quenching. Recent calculations[19] of $HeSr^+$ show that the potential curves are qualitatively very similar to the alkali–noble-gas case, and show no curve crossings at thermal energies. Gallagher[9] measured cross sections for fine-structure mixing in the alkalis, and showed that the cross sections are strongly dependent on the fine-structure splitting. For Cs, with a fine-structure splitting of 554 cm^{-1}, a cross section of 10^{-19} cm^2 was measured at 600 °C. Since the $5\,^2D_{3/2}$ state of Ba^+ has an energy of 4874 cm^{-1}, the cross section for $5\,^2D_{3/2}$ quenching by He should be about a factor of $\exp 4874/554 = 3000$ smaller, consistent with the upper limit obtained here. Thus the probable interpretation of the ion trap experiments is that the quenching is due to impurities, and so the upper limit of $\sigma_{He} < 9\times10^{-22}$ cm^2 of the current experiment is reasonable.

ACKNOWLEDGMENTS

We thank W. Happer, J. Huennekens, and G. Gallup for many useful discussions about this work. We are also grateful to R. Austin for the loan of his Ar^+ laser and dye laser. This work was supported by the Army Research Office Grant No. DAAL03-87-K-0068.

[1] H. L. Chen and G. Erbert, J. Chem. Phys. **78**, 4985 (1983); R. E. Grove, Laser Focus **18**, 45 (1982); K. F. Scheibner, A. U. Hazi, and R. J. W. Henry, Phys. Rev. A **35**, 4869 (1987).
[2] B. G. Bricks, T. W. Karras, and R. S. Anderson, J. Appl. Phys. **49**, 38 (1978).
[3] K. U. Baron and B. Stadler, IEEE J. Quantum Electron. **QE-11**, 852 (1975); V. M. Klimkin, V. N. Nikolaev, V. G. Sokovikov, and V. B. Shcheglov, JETP Lett. **34**, 105 (1981).
[4] T. G. Walker, K. D. Bonin, and W. Happer, J. Chem. Phys. **87**, 660 (1987).
[5] E. Hinnov and W. Ohlendorf, J. Chem. Phys. **50**, 3005 (1969).
[6] Z. Wu, M. Kitano, W. Happer, M. Hou, and J. Daniels, Appl. Opt. **25**, 4483 (1986).
[7] A. Gallagher, Phys. Rev. **157**, 24 (1967).
[8] R. G. Giles and E. L. Lewis, J. Phys. B **15**, 2871 (1982).
[9] A. Gallagher, Phys. Rev. **172**, 88 (1968).
[10] T. B. Reed, *Free Energy of Formation of Binary Compounds* (MIT, Boston, 1971), p. 5.
[11] M. Mitchner and C. H. Kruger, *Partially Ionized Gases* (Wiley, New York, 1973).
[12] M. J. Seaton, in *Atomic and Molecular Processes*, edited by D. R. Bates (Academic, New York, 1962).
[13] D. Petrini, C. R. Acad. Sci. Paris **260**, 4629 (1965).
[14] S. J. Sramek, Phys. Rev. A **22**, 2630 (1980); Although the "excited state" curves reported in this paper have the qualitative appearance of interaction potentials for excited states, they actually are eigenvalues from pseudostates designed to improve the description of the ground state (G. Gallup, private communication).
[15] P. G. Whitkop and J. R. Wiesenfeld, J. Chem. Phys. **72**, 1297 (1980).
[16] P. A. Bokhan, Sov. J. Quantum Electron. **16**, 1207 (1986).
[17] R. O. Jones, J. Chem. Phys. **71**, 1300 (1979).
[18] R. Schneider and G. Werth, Z. Phys. A **293**, 103 (1979).
[19] H. Harima, T. Ihara, Y. Urano, and K. Tachibana, Phys. Rev. A **34**, 2911 (1986).